ISGSR2007 First International Symposium on Geotechnical Safety & Risk
Oct. 18~19, 2007 Shanghai
Tongji University, China

A new reliability-based design approach based on limit-state factor

J. Ching
National Taiwan University of Science and Technology, Taipei

ABSTRACT: Recently, reliability-based design approaches emerge as a more reasonable and rigorous way of handling uncertainties. In particular, design approaches based on load and resistance factors (LRFD methods) are increasingly popular. However, for geotechnical problems, it is sometimes not trivial to discriminate loads from resistances. The implementation of LRFD methods seems problematic for these cases. In this paper, a completely different view is taken for reliability-based design. It is shown that sophisticated reliability-based design can be achieved with a single factor, called the limit-state factor. Moreover, the new approach does not require discrimination between loads and resistances but only requires the knowledge of the limit state function. Even more attractively, simple Monte Carlo simulations are sufficient to calibrate the limit-state factor. Several numerical examples are used to verify the proposed approach. The results show that the proposed approach is quite promising.

1 INTRODUCTION

Uncertainties are abundant in civil engineering systems. Traditionally, geotechnical engineers have been used to design approaches based on safety factors to account for uncertainties due to their simplicity and convenience. However, safety-factor approaches are not rigorous for the purpose. Recently, reliability-based design (Bea et al. 1999; Zhang et al. 2001; Phoon et al. 2003; Chalermyanont and Benson 2004; Low 2005) is popular for quantifying these uncertainties. In particular, load-resistance factor design (LRFD) methods (FHWA 2001; McVay et al. 2003; Paikowsky et al. 2004) are very well known and have been implemented for some geotechnical design problems.

Unlike structural systems, it is sometimes difficult to clearly define the loads and resistances as separate terms for geotechnical systems. As an example, Figure .1 shows a typical design diagram of a sheet-pile wall. As seen in the figure, the active earth pressure of the soil at the right-hand-side of the wall may be interpreted as the loading. However, the passive earth pressure developed in the same soil mass seems to be part of the resistance. Hence, the loading and resistance cannot be treated as separate terms because they are highly correlated. How do we implement LRFD in such a case? This issue is even more pronounced if we consider the consolidation example in Figure .2. Although it is clear that the loading is the force q_0 in the figure, what is the resistance?

The above two examples show that for geotechnical problems, defining loads and resistances is not as easy as for the structural problems. In this research, we take a completely different approach from the LRFD perspective. We show that with a single factor, called the limit-state factor, reliability-based design problem can be easily converted into a design problem similar to safety-factor design. This new approach does not require definitions of loads and resistances: it only requires the definition of limit state. The limit state can be concerning ultimate capacity or serviceability. Moreover, calibrating the limit-state factor only requires simple Monte Carlo simulations, and the approach is applicable to general design problems, e.g.: simple limit-equilibrium design problems or finite-element-based design problems. Several simulated examples will be used to verify the new design approach, where it is seen that the proposed method is very promising.

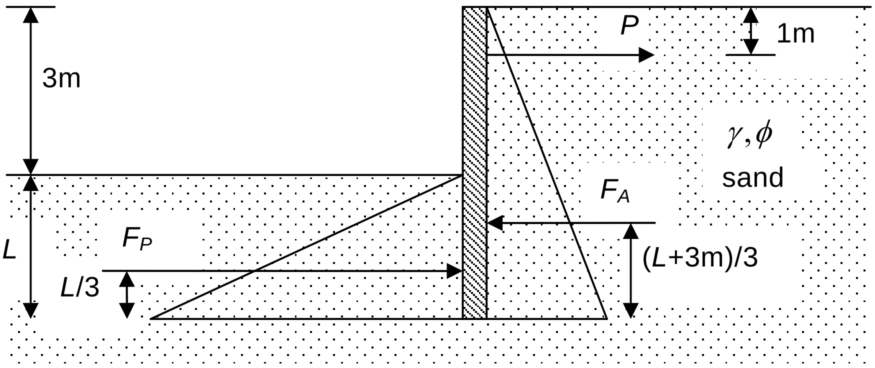

Fig.1 The cross section of the sheet-pile wall

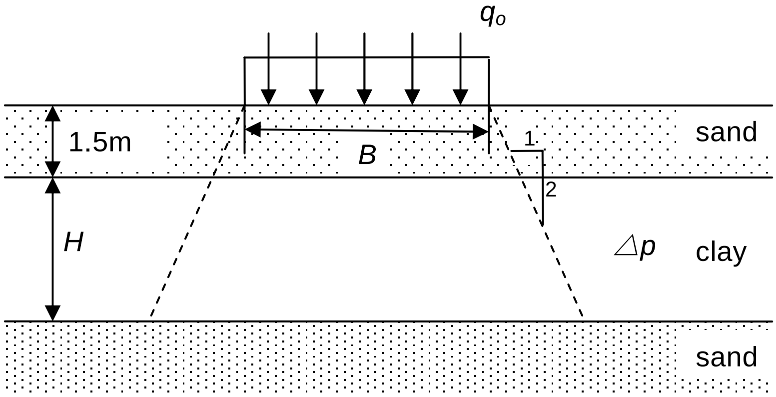

Fig.2 The cross section of the consolidation problem

2 RELIABILITY-BASED DESIGN

Let Z and θ be uncertain variables and design variables (e.g. the penetration depth of the sheet-pile wall) of the target system. Also let *D* be the prescribed allowable design region in the θ space. Let *F* denotes the failure event: $F \equiv \{R[Z,\theta] > 1\}$, where $R[Z,\theta]$ is called the limit-state function. This function does not necessarily define the complete collapse of the system but the performance of the system, e.g. serviceability or ultimate capacity. Throughout the paper, it is assumed without loss of generality that $R[Z,\theta]$ is positive and that the probability density function (PDF) of the uncertainty Z conditioning on θ, denoted by $p(Z \mid \theta)$, is known from site characterization.

The reliability-based design approach is to enforce the following constraint during the design process:

$$P\left(R[Z,\theta] > 1 \middle| \theta\right) = \int p(Z \mid \theta) \cdot I\left(R(Z,\theta) > 1\right) dZ \leq P_F^* \tag{1}$$

where P_F^* is the allowable failure probability; $I(\cdot)$ is the indicator function, i.e. it is equal to 1 if the inside statement is true; otherwise, it is zero.

Let us further define the nominal limit-state function $R_n(\theta)$, a positive function of θ. An example of $R_n(\theta)$ is to take $R[Z,\theta]$ but fix Z at certain chosen nominal values, e.g. their mean values. We propose that (we will prove it later) with certain premise, the reliability-based constraint is identical to the following limit-state constraint:

$$\eta^* \cdot R_n(\theta) \leq 1 \tag{2}$$

for certain carefully chosen η^*, called the limit-state factor. That is, in order to ensure (1) is satisfied during the design process, we only need to make sure (2) is satisfied.

Note that designs based on (2) are convenient since in order to make sure (2) holds, it only requires a single evaluation of $R_n(\theta)$. However, designs based on (1) are more theoretically involved and computationally demanding: in order to verify if (1) holds, it requires a reliability analysis, which may take numerous evaluations of R[Z,θ]. We call the process of determining the relationship between the allowable failure probability P_F^* and the limit-state factor η^* as the process of limit-state-factor calibration. Once this relationship is known (e.g. Figure 3), one can convert the reliability-based design problem (1) into a limit-state design problem (2): given the allowable failure probability P_F^*, one just finds the corresponding safety factor η^* on the curve in Figure 3.

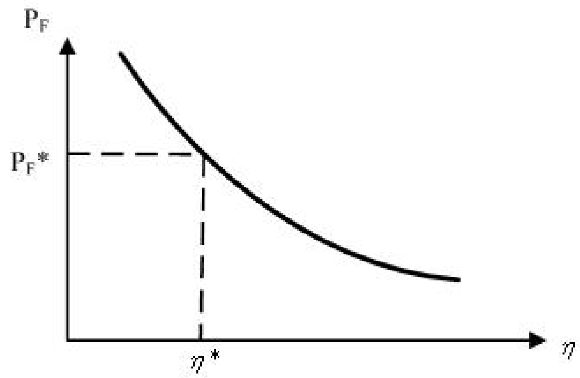

Fig.3 The η^* versus P_F^* relationship

3 MAIN THEOREM

In the following, a fundamental theorem that is central to this research is stated and proved. This theorem proves that under some premise, the two constraints in (1) and (2) are equivalent.

3.1 Theorem – Equivalence between Reliability-based and Limit-state Designs

If the probability distribution of $R[Z,\theta]/R_n(\theta)$ is invariant over the entire allowable design region D, there exists pairs of $[\eta^*, P_F^*]$ such that the two constraints in (1) and (2) are equivalent. Moreover, the functional relationship between the pair $[\eta^*, P_F^*]$ is as follows:

$$P\left(R[Z,\theta] - \eta^* R_n(\theta) > 0\right) = P_F^* \tag{3}$$

where θ is treated as random and uniformly distributed over D.

Let us prove the theorem as follows. First, consider the following proposition:

Proposition: If the distribution of $R[Z,\theta]/R_n(\theta)$ is invariant over the entire allowable design region D, the following two statements are equivalent:

$$P\left(R[Z,\theta] - \eta^* R_n(\theta) > 0\right) = P_F^* \qquad \theta \sim \text{unif}(D)\ (\theta \text{ random}) \tag{4}$$

and

$$P\left(R\left[Z,\theta\right]-\eta^{*}R_{n}\left(\theta\right)>0\mid\theta\right)=P_{F}^{*}\qquad\qquad \forall\,\theta\in D\ (\theta\ \text{deterministic})\tag{5}$$

Proof of the proposition: First note that for (5) to be valid, the premise (the invariance of the distribution of $R[Z,\theta]/R_n(\theta)$ over D) is required. Furthermore,

$$P\left(R\left[Z,\theta\right]-\eta^{*}R_{n}\left(\theta\right)>0\right)=E_{\theta}\left[P\left(R\left[Z,\theta\right]-\eta^{*}R_{n}\left(\theta\right)>0\mid\theta\right)\right]\tag{6}$$

Therefore, (5) clearly implies (4) because

$$P\left(R\left[Z,\theta\right]-\eta^{*}R_{n}\left(\theta\right)>0\right)=E_{\theta}\left[P_{F}^{*}\right]=P_{F}^{*}\tag{7}$$

On the other hand, since $P(R[Z,\theta]-\eta^{*}R_n(\theta)>0|\theta)$ is a constant function of θ on D, it follows that (4) also implies (5).

3.2 Proof of the Main Theorem

First let us call the probability that $R[Z,\theta]-\eta^{*}R_n(\theta)>0$ as P_F^{*}, where θ is treated as random and uniformly distributed over D. Recall that the premise of the theorem is that the distribution of $R[Z,\theta]/R_n(\theta)$ is invariant over D. Under this premise and from the previous proposition, (5) is assured. To demonstrate the equivalence between (1) and (2) under the premise, we may show that under (5), (2) implies (1), and also the negation of (2) implies the negation of (1).

Proof that (2) implies (1): If (2) is true, there must exist $\varepsilon\geqq\tilde{0}$ such that $h^{*}R_n(\theta)+e=1$. Since $P(R[Z,\theta]-\eta^{*}R_n(\theta)>0|\theta)=P_F^{*}$ and $P(R[Z,\theta]>x|\theta)$ is a decreasing function of x,

$$P\left(R\left[Z,\theta\right]>1\mid\theta\right)=P\left(R\left[Z,\theta\right]>\eta^{*}R_{n}\left(\theta\right)+\varepsilon\mid\theta\right)=P\left(R\left[Z,\theta\right]-\eta^{*}R_{n}\left(\theta\right)>\varepsilon\mid\theta\right)\leq P_{F}^{*}\tag{8}$$

Proof that the negation of (2) implies the negation of (1): If (2) is false, there must exist $\tilde{\varepsilon}$ such that $\eta^{*}R_n(\theta)-\varepsilon=1$. Since $P(R[Z,\theta]-\eta^{*}R_n(\theta)>0|\theta)=P_F^{*}$ and $P(R[Z,\theta]>x|\theta)$ is a decreasing function of x, it is clear that

$$P\left(R\left[Z,\theta\right]>1\mid\theta\right)=P\left(R\left[Z,\theta\right]>\eta^{*}R_{n}\left(\theta\right)-\varepsilon\mid\theta\right)=P\left(R\left[Z,\theta\right]-\eta^{*}R_{n}\left(\theta\right)>-\varepsilon\mid\theta\right)>P_{F}^{*}\tag{9}$$

End of the proof. Note that the property that $P(R[Z,\theta]>x|\theta)$ is a decreasing function of x is the key to the proof.

3.3 Discussion of the Theorem

According to the above theorem, the reliability-based design constraint (1) can be transformed into the limit-state design constraint (2) if the distribution of $R[Z,\theta]/R_n(\theta)$ is invariant over D, i.e.: let us denote $S_R\chi\{\theta{:}P(R[Z,\theta]>1|\theta)\leqq P_F^{*}\}$ be the design region that satisfies the reliability-based constraint that failure probability is less or equal to the allowable failure probability P_F^{*}. From the theorem, if the distribution of $R[Z,\theta]/R_n(\theta)$ is indeed invariant over D, it is assured that the region S_R is identical to the following region: $S_L\chi\{\theta{:}\ \eta^{*}R_n(\theta)\leqq 1\}$, where η^{*} can be found by solving (3).

This result is intriguing: it is possible to characterize reliability-based design in (1) with a single limit-state factor in (2). Also, the theorem does not require the definitions of loads and resistances but only require the definition of the limit state. Hence the issues encountered by the two examples in Introduction are eliminated.

Recall that the theorem is based on the premise that the distribution of $R[Z,\theta]/R_n(\theta)$ is invariant over the entire allowable design region D. This can be achieved if the nominal limit-state function

$R_n(\theta)$ is chosen carefully. However, finding such a perfect choice is itself a difficult problem. Although finding the perfect choice is hard, finding a nominal function $R_n(\theta)$ such that the distribution of $R[Z,\theta]/R_n(\theta)$ is roughly invariant is a relatively easy task. As seen in the examples in a later section, $R_n(\theta)=R(E(Z),\theta)$ is usually an acceptable choice. This is because although the distribution of $R[Z,\theta]$ may change dramatically with θ (see Figure 4(a)), the distribution of $R[Z,\theta]/R_n(\theta)$ usually does not (see Figure 4(b)) due to the cancellation effect between $R[Z,\theta]$ and $R_n(\theta)$.

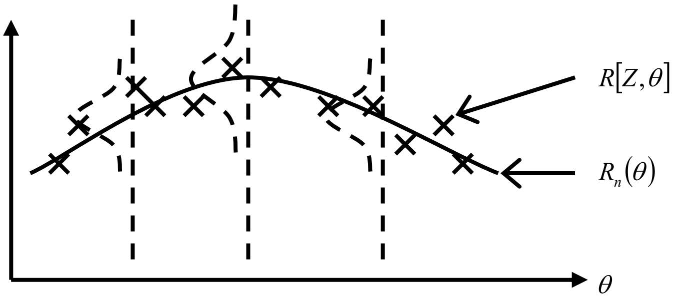

(a) Illustration of the distribution of $R[Z,\theta]$

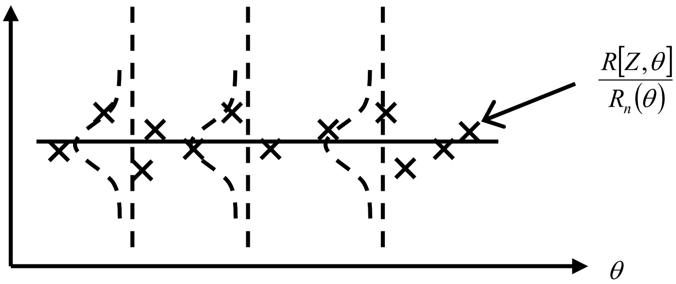

(b) Illustration of the distribution of $R[Z,\theta]/R_n(\theta)$

Fig.4 Illustration of the distributions of $R[Z,\theta]$ and $R[Z,\theta]/R_n(\theta)$

It is desirable to estimate the relationship between η^* and P_F^* through (3) since once this relationship is known for the target system, one can convert the reliability-based design problem into a limit-state design problem. In the next section, algorithms of estimating this functional relationship will be presented.

4 CALIBRATING LIMIT-STATE FACTOR

Calibration of the limit-state factor can be achieved by estimating the η^* and P_F^* relationship in (3), rewritten here as

$$P\left(\frac{R[Z,\theta]}{R_n(\theta)} > \eta^*\right) = P\left(G(Z,\theta) > \eta^*\right) = P_F^* \tag{10}$$

where the normalized limit state $R[Z,\theta]/R_n(\theta)$ has been written as $G(Z,\theta)\chi G$ for convenience. In other words, η^* is simply the 100*(1-P_F^*) percentile of the normalized limit state G.

4.1 Estimating the Relationship with Monte Carlo Simulation

A simple procedure based on Monte Carlo simulation (MCS) can be used to estimate the relationship between η^* and P_F^*: Draw N samples of $[Z,\theta]$, denoted by $\{[Z^{(i)},\theta^{(i)}]:i=1,\ldots,N\}$, where Z samples are drawn from the PDF of Z, and θ samples are drawn from the uniform PDF over D. For a chosen η^* value, the corresponding P_F^* value can be estimated by Law of Large Number:

$$P_F^* \approx \frac{1}{N}\sum_{i=1}^{N} I\left(G\left(Z^{(i)},\theta^{(i)}\right) > \eta^*\right) = \frac{1}{N}\sum_{i=1}^{N} I\left(G^{(i)} > \eta^*\right) \equiv P_F^{MCS*} \tag{11}$$

where $G^{(i)}=G(Z^{(i)},q^{(i)})$. By changing the η^* value, one can find the corresponding P_F^{MCS*} values by repetitively applying (11), i.e. the entire functional relationship between η^* and P_F^* can be obtained. Note that the same N MCS samples can be repetitively used to estimate the entire functional relationship.

P_F^{MCS*} is an unbiased estimator of P_F^*. Its coefficient of variation (c.o.v.) is

$$\delta\left(P_F^{MCS*}\right) = \frac{\sqrt{Var\left[P_F^{MCS*}\right]}}{E\left[P_F^{MCS*}\right]} = \sqrt{\frac{1-P_F^*}{N \cdot P_F^*}} \tag{12}$$

The performance of MCS in estimating the η^* and P_F^* relationship is independent of problem dimension, complexity, and the uncertainty dimension. When the allowable failure probability P_F^* is large, the c.o.v. of P_F^{MCS*} is small, so the afore-mentioned procedure of estimating P_F^* is accurate, but when the allowable failure probability is small, which is usually the case, the procedure requires a large number of samples to make the P_F^* estimates accurate. This is the drawback of MCS: The MCS samples $\{G^{(i)}: i=1,\ldots,N\}$ can only effectively populate the main support region of the PDF of G, denoted by $p(g)$. Unfortunately, in order to estimate the functional relationship between η^* and P_F^* accurately in the small P_F^* region, the tail of $p(g)$ must be well explored, i.e. G samples in the tail region are necessary. Of course, one can obtain these samples by MCS with a very large sample size. However, doing so requires much computation.

4.2 Estimating the Relationship with Subset Simulation

When P_F^* is small, Subset Simulation (SubSim) (Au & Beck 2001, Ching et al. 2005a, Ching et al. 2005b) can be used to estimate the entire η^* and P_F^* relationship more efficiently than MCS. SubSim provides a more efficient way to propagate samples into the tail of the PDF of the quantity of interest. For our purpose, the quantity of interest is exactly G. The first stage of SubSim is an MCS step: draw $[Z,\theta]$ samples $\{[Z^{(i)},\theta^{(i)}]:i=1,\ldots,N\}$ to obtain $\{G^{(i)}: i=1,\ldots,N\}$, i.e. samples from $p(g)$. Note that these samples cannot effectively populate the tail of $p(g)$.

The next step is to choose a threshold b_1. Suppose there are N_1 samples in the left-hand-side of b_1; therefore, $P(G<b_1)$ and $P(G\geqq b_1)$ are roughly N_1/N and $1\text{-}N_1/N$, respectively. The N_1 samples are distributed as $p(g|G<b_1)$, denoted by $\{G^{(i)}_{0\rightarrow 1}:i=1,\ldots,N_1\}$, while the $N\text{-}N_1$ samples in the right-hand-size are distributed as $p(g|G\geqq b_1)$. The $N\text{-}N_1$ samples are used to generate N_1 more samples that are also distributed as $p(g|G\geqq b_1)$ by using the Metropolis-Hastings algorithm (Au and Beck 2001): simply conduct the algorithm with the stationary PDF being $p(g)$ but enforce the acceptance criterion $G\geqq b_1$. Together with the original $N\text{-}N_1$ samples, there are N samples distributed as $p(g|G\geqq b_1)$.

Now the next threshold is chosen to be b_2. Suppose there are N_2 samples in the left-hand-side of b_2; therefore, $P(G<b_2|G\geqq b_1)$ and $P(G\geqq b_2|G\geqq b_1)$ are roughly N_2/N and $1\text{-}N_2/N$, respectively. These N_2 samples are distributed as $p(g|b_1\leqq G<b_2)$, denoted by $\{G^{(i)}_{1\rightarrow 2}:i=1,\ldots,N_2\}$, while the $N\text{-}N_2$ samples in the right-hand-size are distributed as $p(g|G\geqq b_2)$. Then the $N\text{-}N_2$ samples are used to generate N_2 more samples so that there are, again, N samples distributed as $p(g|G\geqq b_2)$. The same procedure is repeated until enough samples have propagated to the desirable tail region of $p(g)$.

Suppose the procedure is repeated for m stages to reach the designated η^*, i.e. $b_m>\eta^*$ while $b_{m\text{-}1}<\eta^*$, the following samples will be available: $\{G^{(i)}_{0\rightarrow 1}:i=1,\ldots,N_1\}$, distributed as $p(g|G<b_1)$, $\{G^{(i)}_{j\rightarrow j+1}:i=1,\ldots,N_{j+1}\}$, distributed as $p(g|b_j\leqq G<b_{j+1})$, for $j=1,\ldots,m\text{-}1$, and $\{G^{(i)}_{m\rightarrow\infty}:i=1,\ldots,N\text{-}N_m\}$, distributed as $p(g|G\geqq b_m)$. Also, the following probability estimates are available: $P(G<b_1)\fallingdotseq N_1/N$, $P(G<b_{j+1}|G\geqq b_j)\fallingdotseq N_{j+1}/N$ $(j=1,\ldots,m\text{-}1)$, and $P(G\geqq b_m|G\geqq b_{m\text{-}1})\fallingdotseq 1\text{-}N_m/N$. One can verify that P_F^* in (10) can be estimated by using the following estimator:

$$
\begin{aligned}
P_F^* &= P\left(G > \eta^*\right) = P\left(G > \eta^* \mid G < b_1\right) P\left(G < b_1\right) \\
&\quad + \sum_{j=1}^{m-1} P\left(G > \eta^* \mid b_j \le G < b_{j+1}\right) P\left(b_j \le G < b_{j+1}\right) + P\left(G > \eta^* \mid G \ge b_m\right) P\left(G \ge b_m\right) \\
&\approx \frac{1}{N}\left(\sum_{i=1}^{N_1} I\left(G_{0\to 1}^{(i)} > \eta^*\right) + \sum_{j=1}^{m-1}\left[\sum_{i=1}^{N_{j+1}} I\left(G_{j\to j+1}^{(i)} > \eta^*\right) \cdot \prod_{n=1}^{j}\left(1-\frac{N_n}{N}\right)\right] + \sum_{i=1}^{N-N_m} I\left(G_{m\to\infty}^{(i)} > \eta^*\right) \cdot \prod_{j=1}^{m-1}\left(1-\frac{N_j}{N}\right)\right) \\
&\equiv P_F^{SS*}
\end{aligned}
\tag{13}
$$

where we have used the fact that

$$
P\left(b_j \le G < b_{j+1}\right) = P\left(G \ge b_1\right) \cdot P\left(G \ge b_2 \mid G \ge b_1\right) \cdots\cdot P\left(G < b_{j+1} \mid G \ge b_j\right) \approx \frac{N_{j+1}}{N} \cdot \prod_{n=1}^{j}\left(1-\frac{N_n}{N}\right) \tag{14}
$$

and that

$$
P\left(G \ge b_m\right) = P\left(G \ge b_1\right) \cdot P\left(G \ge b_2 \mid G \ge b_1\right) \cdots\cdot P\left(G \ge b_m \mid G \ge b_{m-1}\right) \approx \prod_{n=1}^{m}\left(1-\frac{N_j}{N}\right) \tag{15}
$$

By changing the η^* value, one can find the corresponding P_F^{SS*} values by repetitively applying (13), i.e. the entire relationship between η^* and P_F^{SS*} is obtained. Note that the same SubSim samples can be repetitively used to estimate the entire functional relationship. In SubSim, a popular choice is to pick the threshold values $\{b_j{:}j=1,\ldots,m\}$ such that $P(G \geqq b_{j+1}|G \geqq b_j)$ ($j=1,\ldots,m-1$) are all roughly 0.1, or equivalently, to take $N_1=N_2=\ldots=N_m=0.9N$. This can be easily done by adaptively choosing b_j as the 90% percentile among $\{G^{(i)}_{j-1\to j}{:}i=1,\ldots,N_j\}$. The SubSim estimator P_F^* is asymptotically unbiased. The mathematical representation of its c.o.v. can be found in Au and Beck (2001). The performance of SubSim in estimating the η^* and P_F^* relationship is also independent of problem dimension, complexity, and the uncertainty dimension.

5 EXAMPLES

In this section, three examples are investigated to demonstrate the use of the proposed method, including: (a) a sheet-pile wall; (b) a shallow foundation; (c) a consolidation problem. The goal of the examples is to validate the use of the proposed method. In special, the resulting limit-state designs will be compared with the original reliability-based designs. The definition for the failure event F, design variable q and the allowable design region D varies in the examples. All examples are analyzed with MCS with large sample sizes (N = 100,000) because the computation of each limit state is extremely fast. For all examples, the nominal limit-state function is chosen to be $R(E(Z),\theta)$.

5.1 Sheet-pile Wall

This example considers a sheet-pile wall (Figure .1) subject to uncertainties. The uncertain variables Z include the density of the cohesiveless soil γ (Z_1) and its friction angle ϕ (Z_2). All uncertain variables are modelled as independent and normally distributed variables with the mean values equal to $E(Z)$ = [17kN/m^3,40^o] and standard deviations equal to $std(Z)$ = [1.5kN/m^3,2°]. The design parameters considered in this example include the penetration depth L (θ_1) and the anchor force P (θ_2). The design region D is the rectangular region formed by L$\in$[0,3]m and P$\in$[0,30]kN/m.

The first limit state concerns equilibrium of lateral force:

$$
R_1\left(Z,\theta\right) = F_A / \left(F_P + P\right) \tag{16}
$$

where

$$F_A = \frac{1}{2}\gamma(3+L)^2 \tan^2\left(45^o - \frac{\phi}{2}\right) \qquad F_P = \frac{1}{2}\gamma L^2 \tan^2\left(45^o + \frac{\phi}{2}\right) \tag{17}$$

F_A is the active earth force, while F_P is the passive earth force. The second limit state concerns equilibrium of overturning moment:

$$R_2(Z,\theta) = \left(F_A \times \frac{1}{3}(3+L)\right) \Big/ \left(F_P \times \frac{1}{3}L + P(2+L)\right) \tag{18}$$

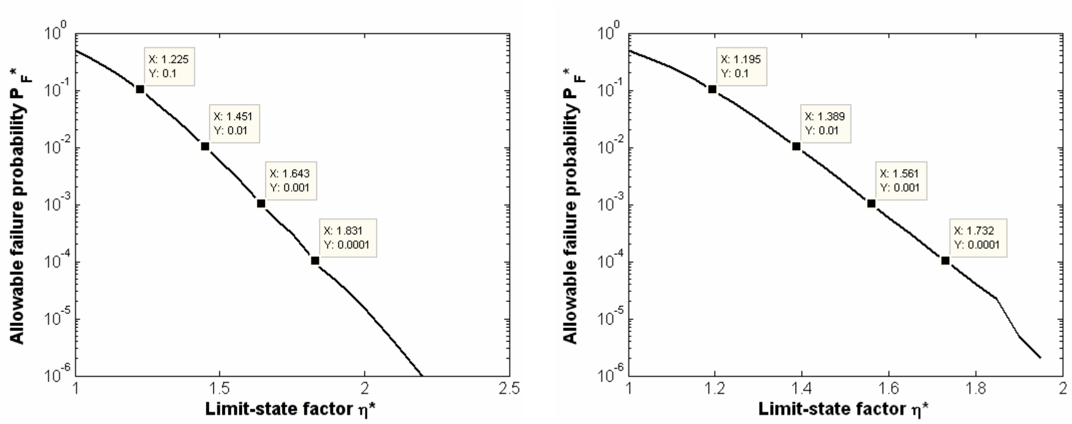

(a) First limit state (b) Second limit state

Fig.5 The estimated η^* vs. P_F^* relationship for the two limit states of Example 1. The η^* corresponding to P_F^* = 0.1, 0.01, 0.001, and 0.0001 are tabulated in the figures

The estimated η^* vs. P_F^* relationship is shown in Figure 5. To examine the results in the figure, the following approach is taken: In the allowable region D, each of the coordinate axes is discretized into discrete points, creating grid points in D. MCS with a very large sample size is then conducted at each of the grid points, giving each point an individual failure probability estimate $P(F|\theta) = P(R(Z,\theta)>1|\theta)$. If the estimated failure probability at a grid point is less than P_F^*, it is marked with label O, otherwise, it is marked with label ×. Therefore, the region occupied by label O should be close to the allowable reliability-based design set $S_R=\{\theta:P(R[Z,\theta]>1|\theta) \leqq P_F^*\}$.

On the other hand, for the chosen P_F^*, the corresponding η^* is identified from Figure 5, and the allowable limit-state design set $S_L=\{\theta:\eta^* R_n(\theta) \leqq 1\}$ is plotted as the shaded region in Figures .6 and .7. Such comparisons are conducted for several chosen $[\eta^*, P_F^*]$ pairs. It can be seen that the two sets match each other very well. This indicates that the resulting limit-state design is indeed very close to the reliability-based design.

To explain how the analysis result can be implemented in actual reliability-based designs, let us consider designing the sheet-pile wall with allowable lateral failure probability equal to 10^{-3} and allowable overturning probability equal to 10^{-2}. Based on the estimated relationship in Figure 5, the corresponding limit-state factors are 1.643 and 1.561 for the two limit states. As a result, one needs only to check if the design satisfies $1.643R_1(\mathrm{E(Z)},\theta) \leqq 1$ and $1.561R_2(\mathrm{E(Z)},\theta) \leqq 1$. If so, we are assured that the desired reliability-based design is achieved.

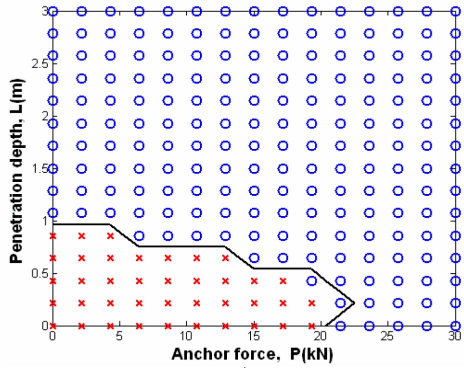

(a) $P_F^* = 0.1$

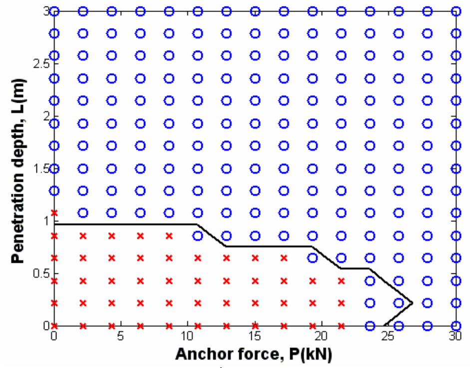

(b) $P_F^* = 0.01$

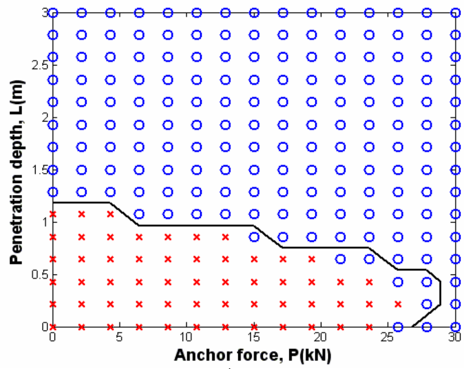

(c) $P_F^* = 0.001$

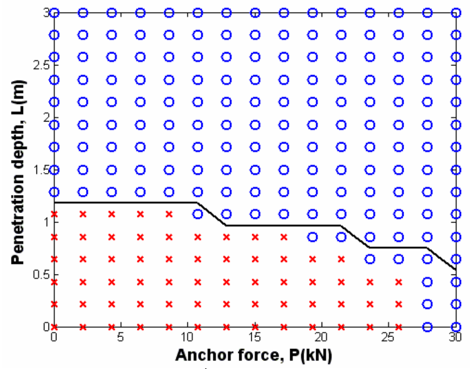

(d) $P_F^* = 0.0001$

Fig.6 Examining results for the first limit state of Example 1. Region 'x' and 'o' is where the failure probability is larger and smaller, respectively, than P_F^*. Solid line is the boundary $\eta^* R_n(\theta)=1$

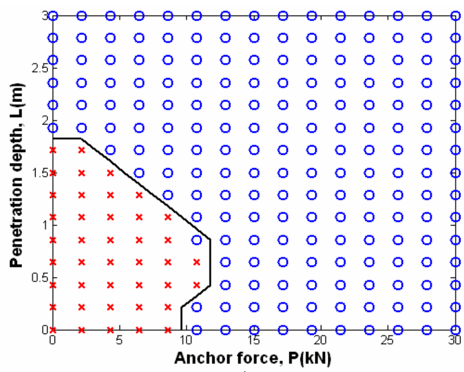

(a) $P_F^* = 0.1$

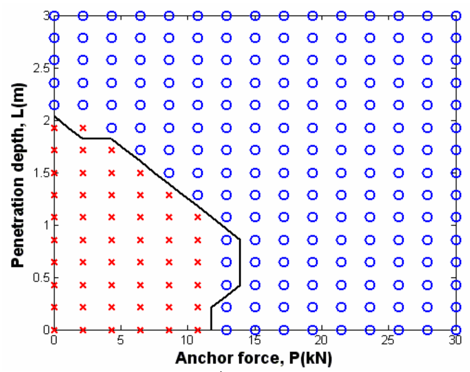

(b) $P_F^* = 0.01$

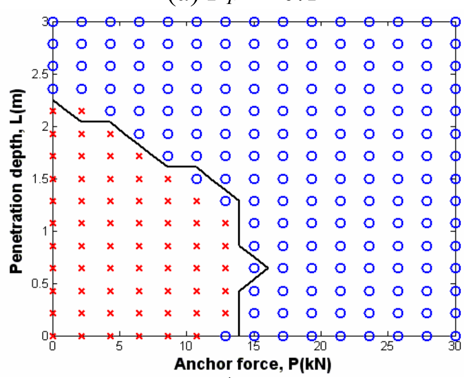

(c) $P_F^* = 0.001$

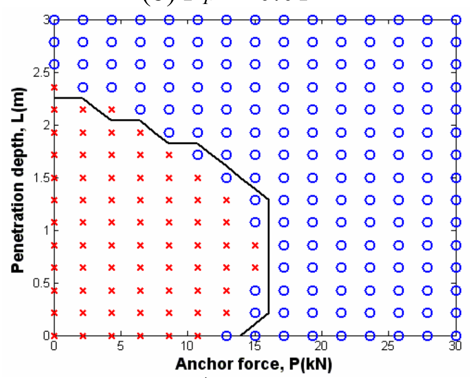

(d) $P_F^* = 0.0001$

Fig.7 The examining results for the second limit state of Example 1

5.2 Shallow Foundation

This example considers a shallow foundation (Figure .8) subject to uncertainties. The uncertain variables Z include the unit weight of the cohesiveless soil γ (Z_1), its friction angle ϕ (Z_2), the total bearing stress q (Z_3), and the inclination angle of ψ (Z_4). The design parameters considered in this example include the depth of foundation D_f (θ_1) and the mean value μ of the inclination angle ψ (θ_2). The design region D is the rectangular region formed by $D_f \in [1\ 2]m$ and $\mu \in [5\ 15]^o$. All uncertain variables are modelled as independent and normally distributed variables with the mean values equal to $E(Z)$=[17kN/m^3,40^o,300kN,μ^o] and standard deviations equal to $std(Z)$=[1.5kN/m^3,2°,60kN,0.1μ^o]. The width of foundation B is 2m.

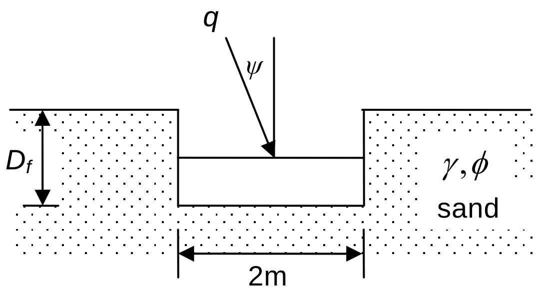

Fig.8 The cross section of the shallow foundation.

The only limit state considered here is the ultimate bearing capacity:

$$R(Z,\theta) = q\cos\Psi / q_u \tag{19}$$

Where

$$q_u = 0.5\gamma B N_r \xi_{\gamma i}\xi_{\gamma d} + \gamma D_f N_q \xi_{qi}\xi_{qd} \qquad N_q = e^{\pi\tan\phi}\tan^2\left(45^o + \frac{\phi}{2}\right) \qquad N_\gamma = 2\left(N_q + 1\right)\tan\phi$$

$$\xi_{\gamma i} = \left(1-\tan\Psi\right)^3 \qquad \xi_{qi} = \left(1-\tan\Psi\right)^2 \qquad \xi_{qd} = 1 + 2\tan\phi\left(1-\sin\phi\right)^2\tan^{-1}\left(\frac{D_f}{B}\right) \tag{20}$$

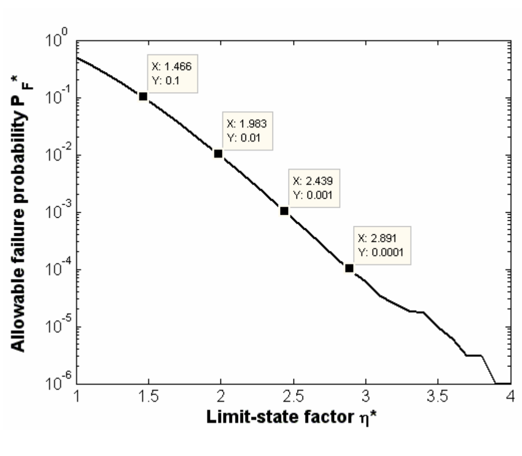

Fig.9 The estimated η^* vs. P_F^* relationship for the limit state of Example 2

The estimated η^* vs. P_F^* relationship is shown in Figure 9. The same examining approach adopted in Example 1 is taken to verify this relationship. Figure .10 show the comparison of the allowable reliability-based design regions S_R and the limit-state design regions S_L. It can be seen that the two sets match each other very well. This indicates that the resulting limit-state design is indeed very close to the reliability-based design.

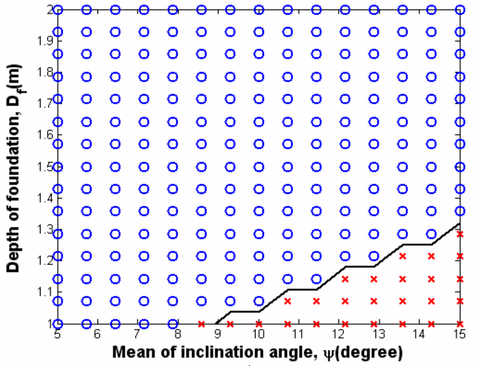

(a) $P_F^* = 0.1$

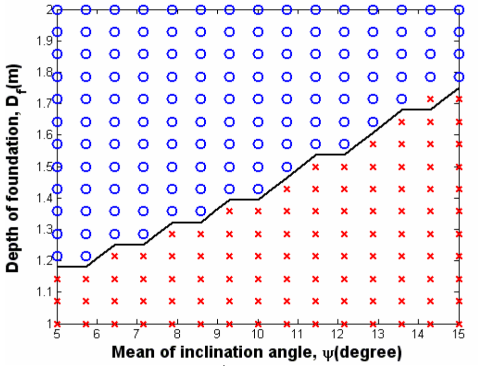

(b) $P_F^* = 0.01$

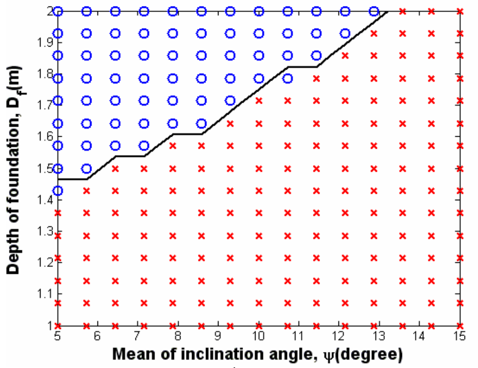

(c) $P_F^* = 0.001$

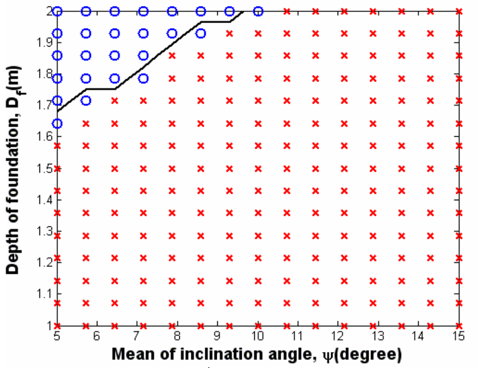

(d) $P_F^* = 0.0001$

Fig.10 The examining results for the limit state of Example 2

5.3 Consolidation Problem

This example considers a consolidation problem (Figure .2). The uncertain variables Z include the thickness of the clayey soil H (Z_1), in-situ consolidation pressure p_0 (Z_2), compression index C_c (Z_3), initial void ratio e_0 (Z_4), the ratio between compression and swelling indices $\alpha = C_r/C_c$ (Z_5) and the over consolidation ratio OCR (Z_6). All uncertain variables are modelled as independent. Z_1 and Z_2 are normally distributed variables with the mean values equal to $E(Z_1,Z_2)$ = [4m,180kPa] and standard deviations equal to $std(Z_1,Z_2)$ = [0.2m,9kPa]. Z_3 and Z_4 are lognormally distributed variables with mean values equal to $E(Z_3,Z_4)$ = [0.4,1.2] and standard deviations equal to $std(Z_3,Z_4)$ = [0.1,0.18]. Z_5 and Z_6 are uniformly distributed variables in the intervals of [0.1,1] and [0.2,1.5], respectively. The thickness of the sand soil is 1.5m. The design parameters considered in this example include the mean value μ of the bearing pressure q_0 (θ_1) and the width of the foundation B (θ_2). The design region D is the region formed by $\mu \in [50, 100]$kPa and $B \in [1,3]$m.

The considered limit state defines the failure event as the total settlement greater than 5cm:

$$R(Z,\theta) = S_c/0.05 \tag{21}$$

where

$$S_c = \begin{cases} C_r H/(1+e_0)\log(p_c/p_0) + C_c H/(1+e_0)\log([p_0+\Delta p]/p_c) & \text{if} \quad p_0+\Delta p > p_c \\ C_r H/(1+e_0)\log([p_0+\Delta p]/p_0) & \text{if} \quad p_0+\Delta p < p_c \end{cases}$$

$$\Delta p = \frac{1}{6}\left(\frac{B\cdot q_0}{B+1.5} + \frac{4B\cdot q_0}{B+0.5H+1.5} + \frac{B\cdot q_0}{B+H+1.5}\right) \qquad p_c = OCR\cdot p_0 \tag{22}$$

p_c is the pre-consolidation stress; Δp is the average stress increment in the clayey soils, determined with the 2:1 method.

The estimated η^* vs. P_F^* relationship is shown in Figure .11. The same examining approach adopted in Example 1 is taken to verify this relationship. Figure .12 show the comparison of the allowable reliability-based design regions S_R and the limit-state design regions S_L. It can be seen that the two sets match each other very well. This indicates that the resulting limit-state design is indeed very close to the reliability-based design.

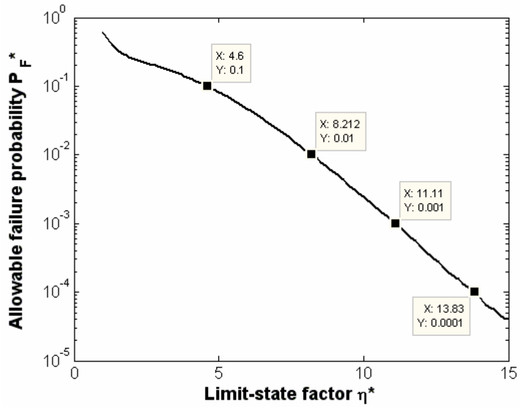

Fig.11 The estimated η^* vs. P_F^* relationship for the limit state of Example 3

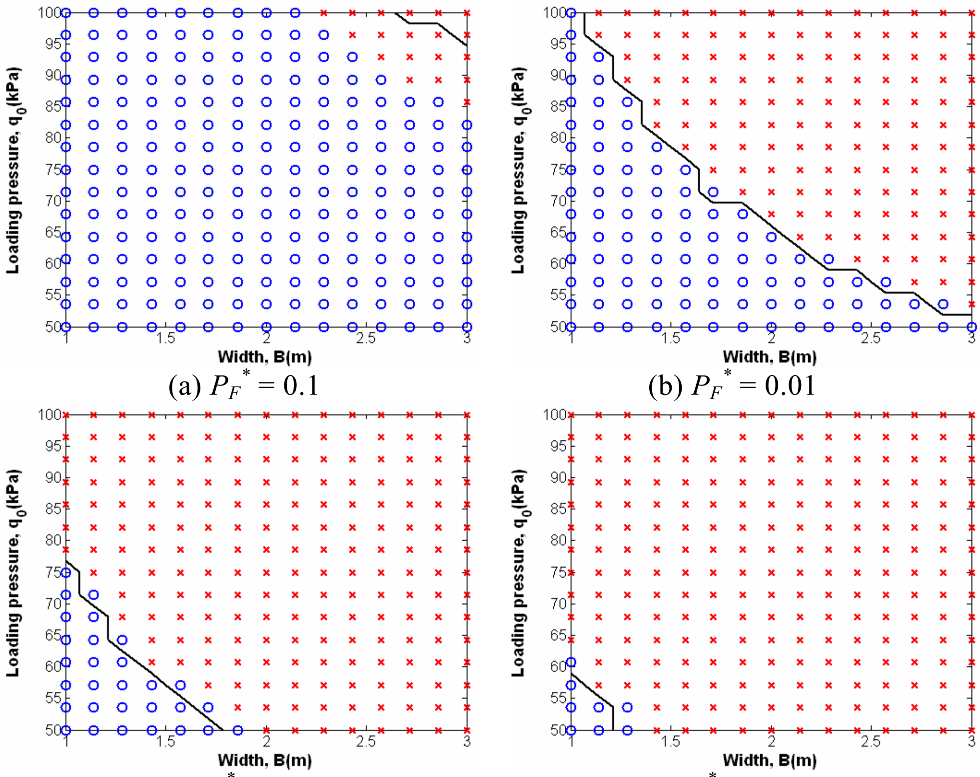

(a) $P_F^* = 0.1$ (b) $P_F^* = 0.01$

(c) $P_F^* = 0.001$ (d) $P_F^* = 0.0001$

Fig.12 The examining results for the limit state of Example 3

6 CONCLUSION

This research shows that under the situation that the definitions of loads and resistances are unclear, it is still possible to achieve reliability-based design by considering the so-called limit-state factors. Moreover, the relationship between allowable failure probability and limit-state factor can be determined via simple Monte Carlo simulation or, when small failure probability is of concern, Subset Simulation. It is observed from the examples that the resulting limit-stat designs are very close to the original reliability-based designs. The impact of this research may be significant: once the relationship between allowable failure probability and limit-state factor is determined, one can achieve a reliability-based design by using a limit-state design approach.

ACKNOWLEDGEMENTS The author greatly appreciates the help from Prof. Kok-Kwang Phoon in providing the examples.

References

Au, S.K. and Beck, J.L. (2001). Estimation of small failure probability in high dimensions by subset simulation. Probabilistic Engineering Mechanics, 16, 263-277.

Bea RG, Jin Z, Valle C, Ramos R. (1999). "Reliability-based design for internal stability of mechanically stabilized earth walls", ASCE Journal of Geotechnical and GeoEnvironmental Engineering, 125(8), 696-704.

Chalermyanont T and Benson CH (2004). "Reliability-based design for internal stability of mechanically stabilized earth walls", ASCE Journal of Geotechnical and GeoEnvironmental Engineering, 130(2), 163-173.

Ching, J., Au, S.K., and Beck, J.L. (2005a). Reliability estimation for dynamic systems subject to stochastic excitations using Subset Simulation with splitting. Computer Methods in Applied Mechanics and Engineering, 194, 1557-1579.

Ching, J., Beck, J.L., and Au, S.K. (2005b). Hybrid Subset Simulation method for reliability estimation of dynamic systems subject to stochastic excitations. Probabilistic Engineering Mechanics, 20, 199-214.

FHWA (2001). Load and resistance factor design for highway bridge substructures, Publication# FHWA HI-98-032, Federal Highway Administration, US Department of Transportation, May 2001.

Low BK (2005). "Reliability-based design applied to retaining walls", Geotechnique, 55(1), 63-75.

McVay M, Kuo C, Guisinger AL (2003). Calibrating resistance factors for load and resistance factor design for statnamic load testing, Final Report # 4910-4504-823-12, Florida Department of Transportation, March 2003.

Paikowsky SG, Birgisson B, McVay M, Nguyen T, Kuo C, Baecher G, Ayyub B, Stenersen K, O'Malley K, Chernauskas L, O'Neill M (2004). Load and Resistance Factor Design (LRFD) for Deep Foundations, NCHRP Report 507, Transportation Research Board, Washington, 2004.

Phoon KK, Kulhawy FH, Grigoriu MD (2003). Development of a reliability-based design framework for transmission line structure foundations. ASCE Journal of Geotechnical and Geoenvironmental Engineering, 129(9): 798-806.

Zhang LM, Tang WH, and Ng CWW (2001). "Reliability of axially loaded driven pile groups", ASCE Journal of Geotechnical and GeoEnvironmental Engineering, 127(12), 1051-1060.